Bioorganic & Medicinal Chemistry 21 (2013) 1756–1763

Contents lists available at SciVerse ScienceDirect

Bioorganic & Medicinal Chemistry

journal homepage: www.elsevier.com/locate/bmc

Design, structure–activity relationship and in vivo efficacy of piperazine analogues of fenarimol as inhibitors of *Trypanosoma cruzi*

Martine Keenan [a,*], Paul W. Alexander [a], Hugo Diao [a], Wayne M. Best [a], Andrea Khong [b,†], Maria Kerfoot [b], R. C. Andrew Thompson [b], Karen L. White [c], David M. Shackleford [c], Eileen Ryan [c], Alison D. Gregg [c], Susan A. Charman [c], Thomas W. von Geldern [d], Ivan Scandale [d], Eric Chatelain [d]

[a] *Epichem Pty Ltd, Murdoch University Campus, South Street, Murdoch, Western Australia 6150, Australia*
[b] *Department of Parasitology and Veterinary Sciences, Murdoch University, South Street, Murdoch, Western Australia 6150, Australia*
[c] *Centre for Drug Candidate Optimisation, Monash Institute of Pharmaceutical Sciences, 381 Royal Parade, Parkville, Victoria 3052, Australia*
[d] *Drugs for Neglected Diseases initiative (DNDi), 15 Chemin Louis Dunant, 1202 Geneva, Switzerland*

ARTICLE INFO

Article history:
Received 15 November 2012
Revised 16 January 2013
Accepted 23 January 2013
Available online 31 January 2013

Keywords:
Trypanosoma cruzi
Chagas disease
Fenarimol
Inhibition

ABSTRACT

A scaffold hopping exercise undertaken to expand the structural diversity of the fenarimol series of anti-*Trypanosoma cruzi* (*T. cruzi*) compounds led to preparation of simple 1-[phenyl(pyridin-3-yl)methyl]piperazinyl analogues of fenarimol which were investigated for their ability to inhibit *T. cruzi* in vitro in a whole organism assay. A range of compounds bearing amide, sulfonamide, carbamate/carbonate and aryl moieties exhibited low nM activities and two analogues were further studied for in vivo efficacy in a mouse model of *T. cruzi* infection. One compound, the citrate salt of **37**, was efficacious in a mouse model of acute *T. cruzi* infection after once daily oral dosing at 20, 50 and 100 mg/kg for 5 days.

1. Introduction

Chagas disease, caused by the protozoan parasite *Trypanosoma cruzi*, is a major neglected parasitic disease endemic in South and Central America with an increasing number of cases reported in countries such as USA, Spain and Japan.[1,2] Research into new therapies to treat Chagas disease must overcome a number of difficulties arising from the complex nature of the parasite's life cycle[3] and its extensive impact on the body.[4] Following infection with *T. cruzi* parasites, blood-form trypomastigotes enter cells and rapidly proliferate in amastigote form, causing acute illness with mild symptoms lasting for a few weeks. Treatment is effective at this point in 60–85% of cases,[5] but acute infection can also cause mortality in a small number of patients.[6] Parasites remain in the body as the disease progresses to an asymptomatic phase during which time patients may not be aware they are carriers of the parasite and may never develop the chronic form of the disease. Chronic Chagas disease can take as long as 15–20 years to present, during which time the amastigote form of *T. cruzi* has caused considerable damage to the heart and/or gastrointestinal tract via infiltration of soft tissues and stimulation of immune responses.[7] A recent epidemiological study of mortality related to Chagas disease in Brazil between 1999 and 2007 reported 97% of diagnosed Chagas related deaths were due to the chronic form of the disease.[6] *T. cruzi* is genetically highly diverse and is divided into six discrete typing units (DTUs)[8] which have the potential to vary in susceptibility to drug treatment. The current standard of care, benznidazole, is given at a high dose for 30–60 days, has undesirable side effects leading to poor patient compliance and has a limited and controversial impact against chronic Chagas disease.[5] The protracted nature of the illness, extent of parasite distribution into the body, monitoring of disease progression and determination of cure add complexity to clinical evaluation of existing and promising new treatments.[1,5]

CYP51 is a well-validated drug target for the inhibition of *T. cruzi* and a major drug target in the cytochrome P450 family.[9] The enzyme is an important part of sterol biosynthesis in eukaryotes, with inhibition causing a breakdown in membrane structural integrity, fluidity and permeability leading to deleterious downstream effects.[10] Pioneering work by Urbina et al. brought antifungal CYP51 inhibitors to the forefront of *T. cruzi* drug discovery

* Corresponding author. Tel.: +61 8 9360 7216; fax: +61 8 9360 7699.
E-mail address: martine.keenan@epichem.com.au (M. Keenan).
† Current address: School of Medicine and Pharmacology, The University of Western Australia, Nedlands 6009, Western Australia.

0968-0896/$ - see front matter © 2013 Elsevier Ltd. All rights reserved.
http://dx.doi.org/10.1016/j.bmc.2013.01.050

establishing the cross-reactivity of leading azole antifungal sterol biosynthesis inhibitors against *T. cruzi* in vitro and in vivo.[11–14] More active second generation antifungals posaconazole and a ravuconazole pro-drug are the first compounds to enter clinical trials for the treatment of Chagas disease in more than 40 years. Other compounds targeting *T. cruzi* CYP51 include the tipifarnib series,[15–18] dialkyl imidazoles,[19] LP10,[20] and indomethacin amides,[21] with current hit generation efforts potentially fueling further research.[22] The recently reported crystal structure of *T. cruzi* CYP51 with bound posaconazole and fluconazole is an important step forward in the ongoing story of this target opening up the opportunity for structure based drug design to address potential issues of drug resistance.[23,24]

We recently identified fenarimol (**1**), a fungicide used in agriculture since the mid-1970s, as having moderate in vitro activity against *T. cruzi* (IC_{50} 350 nM) following a targeted hit generation campaign[25] utilizing a phenotypic whole organism in vitro screen.[26] Fenarimol inhibits fungal CYP51 and is classified within the pyrimidine sub-class of fungal CYP51 inhibitors.[27] The ability of **1** to kill *T. cruzi* could occur by a similar mechanism and the outcome of mechanistic studies will be reported in due course. Structure–activity relationship (SAR) studies focused on improving potency and establishing in vivo efficacy arrived at optimised triaryl analogue **2**, which was orally active in a stringent in vivo mouse model of acute *T. cruzi* infection. In a general effort to expand the chemical diversity of the fenarimol series and assess the subsequent impact of a scaffold hop on activity, selectivity over CYP3A4, solubility, oral exposure and ultimately in vivo efficacy, one aromatic ring of the triaryl pharmacophore of **1** and **2** was replaced with piperazine to give a new 1-(diarylmethyl)piperazinyl scaffold (**3**) which could be further derivatised on the piperazine N-4 atom (Fig. 1).

2. Materials and methods

2.1. Chemistry

The retro synthesis of scaffold **3** is illustrated in Scheme 1. Benzophenones (**8**) were selected as convenient precursors due to their ease of synthesis from classical Friedel–Craft reactions, palladium catalysed acylations or addition of aryl organometallic reagents to Weinreb amide derivatives of carboxylic acids.[25] Straightforward reduction with sodium borohydride gave diarylmethanols (**6**) which were also prepared directly in gram quantities by addition of aryl Grignard or aryllithium species to aromatic aldehydes at low temperature. As both aromatic groups could be introduced as either the organometallic or aldehyde entity, the choice of reacting partners was determined by availability of reagents and reactivity of pendent substituents. Conversion of **6** to the corresponding chloro derivative **7** on reaction with thionyl chloride was followed by substitution with *t*-butyl piperazine-1-carboxylate to give BOC-protected scaffold-**4**. Simple acid mediated deprotection gave **5** in overall good yields.

Reaction of **5** with acid chlorides gave piperazinyl-amide analogues **13–27**; with sulfonyl chlorides gave piperazinyl-sulfonamide analogues **28–42**; isocyanates gave piperazinyl–carbamates **44**,**45, 47, 48, 51, 53–56** and chloroformates gave piperazinyl–carbonates **43, 46, 49, 50** and **52**. Chloro intermediate **7** was also reacted with pre-functionalised piperazine analogues to give the desired target analogues of **3** directly and to prepare R^1 = aryl analogues **57–66**. As representative examples of the synthetic methodology, Schemes 2 and 3 show the preparation of [4-chlorophenyl(pyridin-3-yl)methyl]piperazine analogues **24, 29, 46–47** and **62**, respectively. Compounds were prepared in racemic form and synthetic transformations are unoptimised.

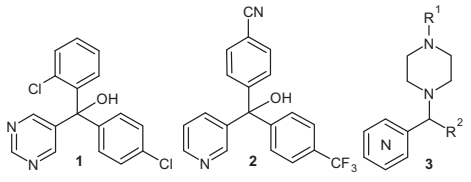

Figure 1. Fenarimol (**1**), **2** and proposed scaffold (**3**).

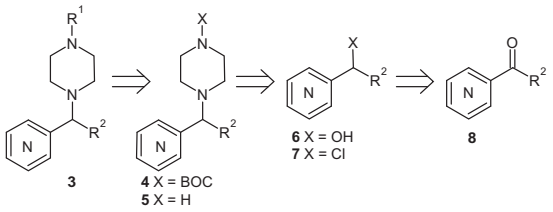

Scheme 1.

2.2. Biological evaluation

The new [phenyl(pyridin-3-yl)methyl]piperazinyl derivatives **13–66** were tested for their ability to inhibit *T. cruzi* in vitro in a whole parasite assay. Specifically, compounds were incubated with *T. cruzi* Tulahuen strain TcVI (a strain transfected with the β-galactosidase gene).[26] Parasites in the extra cellular trypomastigote form were added to the plate wells seeded with L6 cells (rat skeletal myoblasts) and incubated for 48 h to allow infection to establish before addition of test compounds and a further 4-day incubation period, exposing compounds to both the extracellular trypomastigote and intracellular amastigote forms of the parasite. An IC_{50} value was recorded corresponding to the concentration of compound required to inhibit 50% of parasite growth. Compound cytotoxicity was evaluated in L6-cells as a counter-screen. The compounds in this series were determined to be non-cytotoxic with selectivity ratios for *T. cruzi*/cytoxicity generally >100.

Compounds with good activity or those of structural interest were further evaluated for their propensity to undergo in vitro oxidative metabolism by hepatic microsomes and to inhibit CYP3A4, a key drug metabolising enzyme inhibited by most azole-derived CYP51 antifungals. Solubility in phosphate buffer at pH 6.5 was also determined.

Suitable compounds with low to moderate predicted hepatic extraction ratios (Eh) were further evaluated in vivo by measurement of the oral exposure in non-infected Swiss outbred mice and subsequently, for in vivo efficacy in a mouse model of acute *T. cruzi* infection.[25]

3. Results and discussion

The exploration of the SAR was greatly facilitated by the tractable synthesis of the target compounds allowing each region of the pharmacophore to be investigated independently (Fig. 2).

3.1. Structure–activity relationship (SAR)

Exploration of the heterocycle and aromatic ring R^2 was guided by the results of previous SAR studies on the triaryl series, which had established 3-pyridyl and a handful of 4-substituted phenyl motifs as optimal for activity and in vitro oxidative metabolic stability (and thus oral exposure).[25] 5-Pyrimidinyl analogues of several compounds were made in this study in order to confirm that

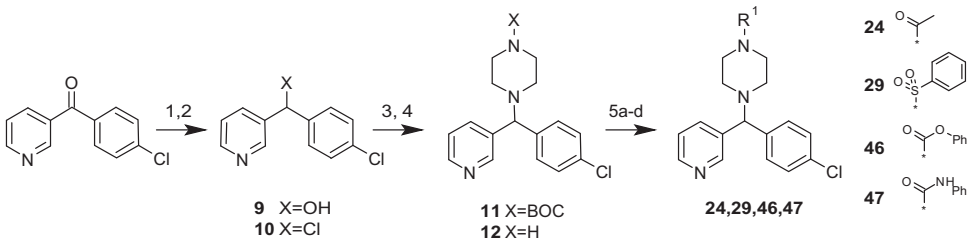

Scheme 2. (1) $NaBH_4$, MeOH, RT, 48 h, (97%); (2) **9**, $SOCl_2$, Tol, reflux, 18 h, (94%); (3) **10**, BOC-piperazine, NEt_3, KI, AcCN, 80 °C, 48 h, (80%). (4) **11**, TFA, DCM, MeOH, rt, 18 h, (quant.) (5) (a) **12**, CH_3COCl, DCM, Et_3N, 0 °C–RT, 1 h, (17%), (b) **12**, $PhSO_2Cl$, DCM, Et_3N, 0 °C–rt, 2 h (83%), (c) **12**, PhOCOCl, DCM, Et_3N, 0 °C–rt, 12 h (56%), (d) **12**, PhN=C=O, DCM, Et_3N, 0 °C–rt, 45 min, (70%).

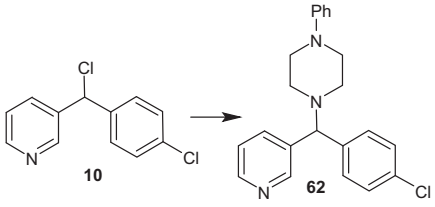

Scheme 3. 10, 1-phenylpiperazine, DMF, K_2CO_3, 150 °C, microwave, 30 min (24%)

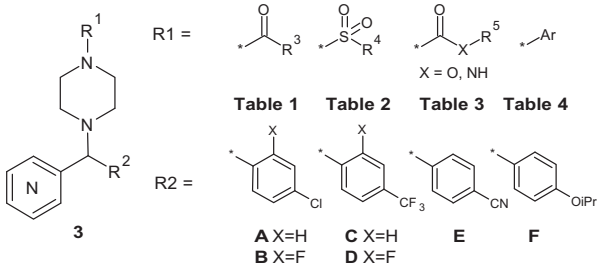

Figure 2. Scope of SAR investigation.

SAR trends remained true in the new piperazine series. The bulk of the SAR exploration was thus focused on establishing the best R^1 group.

In general, across all variations of R^1, the in vitro activity of the new piperazinyl compounds was very encouraging with activities in the low nM range. Tables 1–4 show selected analogues from the amide series (Table 1), sulfonamide series (Table 2), carbamate/carbonate series (Table 3) and aryl series (Table 4). The compounds are ordered by in vitro activity starting with the most active analogue and a twofold difference in IC_{50} value was considered to reflect an actual difference in potency. Activity data for reference compounds posaconazole and benznidazole has been included in Table 1. Posaconazole is very active in vitro, in contrast to the μM activity level of benznidazole.

Considering each different R^1 in turn, for R^1 equal to amide (Table 1) bulky alkyl amido analogues **13–18** were more potent than benzamides **20** and **21**. Thiazole **19** showed good activity. Pyrimidinyl analogues were less potent than the corresponding pyridyl compounds (e.g., **15** *cf* **23**) and there was a slight preference for 2-F containing R^2 analogues (B and D) and a definite mismatch with R^2 = 4-benzonitrile (E).

In contrast, the sulfonamide series (Table 2) showed a preference for aryl sulfonamides over alkyl analogues, and simple benzenesulfonamides **28** and **29** were very active. Additional Cl or *i*Pr substituents did not enhance activity. Methyl sulfonamides **34, 35** and **37–42** provided an interesting sub-set of analogues with surprisingly active and equipotent pyridyl and pyrimidinyl lead compounds, and a clear preference for 2-F containing R^2 analogues B and D (**34** cf. **41** and **35** cf. **38**). Similar to the sulfonamide

Table 1
R^1 = alkyl and aryl amide (COR^3)

Cmpd	HET[a]	R^{2b}	R^3	Tc IC_{50}[c] (μM)	L6 IC_{50}[d] (μM)
13	3-Pyr	B	*t*Bu	0.019	60
14	3-Pyr	D	*t*Bu	0.024	73
15	3-Pyr	B	*c*Pr	0.026	>100
16	3-Pyr	B	*c*Hex	0.028	62
17	3-Pyr	C	*t*Bu	0.030	59
18	3-Pyr	F	*i*Pr	0.035	>100
19	3-Pyr	B	Het[e]	0.036	93
20	3-Pyr	A	Ph	0.068	61
21	3-Pyr	B	Ph	0.070	69
22	5-Pyrim	B	*t*Bu	0.081	>100
23	5-Pyrim	B	*c*Pr	0.171	>100
24	3-Pyr	A	Me	0.240	>100
25	3-Pyr	E	*t*Bu	0.254	>100
26	3-Pyr	E	*c*Pr	0.281	>100
27	3-Pyr	E	Het[e]	0.513	>100
[f]Posa				0.0007	>100
[g]Bnz				1.15	>100

[a] HET: 3-pyr (3-pyridine), 5-pyrim (5-pyrimidine).
[b] A (4-chlorophenyl), B (4-chloro-2-fluorophenyl), C (4-trifluoromethylphenyl), D (2-fluoro-4-trifluoromethylphenyl), E (4-benzonitrile), F (4-*i*propoxyphenyl).
[c] Tc = *T. cruzi*, values are the mean of at least two experiments.
[d] L6 cells (rat myoblasts from skeletal muscle) for assessment of cytotoxicity.
[e] **19**, **27** Het = 2-(4-methyl-1,3-thiazole).
[f] Posa (posaconazole).
[g] Bnz (benznidazole).

Table 2
R^1 = alkyl and aryl sulfonamide (SO_2R^4)

Cmpd	HET[a]	R^{2b}	R^4	Tc IC_{50}[c](μM)	L6 IC50[d] (μM)
28	3-Pyr	B	Ph	0.008	42
29	3-Pyr	A	Ph	0.009	43
30	3-Pyr	A	*c*Hex	0.010	56
31	3-Pyr	A	Ph(4-*i*Pr)	0.012	80
32	5-Pyrim	B	Ph(4-iPr)	0.018	>100
33	3-Pyr	A	Ph(4-Cl)	0.024	23
34	5-Pyrim	D	Me	0.025	>100
35	3-Pyr	D	Me	0.028	77
36	3-Pyr	A	iPr	0.028	>100
37	3-Pyr	B	Me	0.035	>100
38	3-Pyr	C	Me	0.077	>100
39	3-Pyr	A	Me	0.110	>100
40	3-Pyr	E	Me	0.365	>100
41	5-Pyrim	C	Me	0.769	>100
42	5-Pyrim	A	Me	0.880	>100

[a] HET: 3-pyr (3-pyridine), 5-pyrim (5-pyrimidine).
[b] A (4-chlorophenyl), B (4-chloro-2-fluorophenyl), C (4-trifluoromethylphenyl), D (2-fluoro-4-trifluoromethylphenyl), E (4-benzonitrile), F (4-*i*propoxyphenyl).
[c] Tc = *T. cruzi*, values are the mean of at least two experiments.
[d] L6 cells (rat myoblasts from skeletal muscle) for assessment of cytotoxicity.

Table 3
R^1 = alkyl and aryl carbonates/carbamates (COXR^5 X=O/NH)

Cmpd	HET[a]	R^{2b}	R^5	Tc IC_{50}[c] (μM)	L6 IC_{50}[d] (μM)
43	3-Pyr	B	OPh	0.005	59
44	5-Pyr	B	NHPh	0.006	45
45	5-Pyrim	B	NHPh(4-*i*Pr)	0.007	62
46	3-Pyr	A	OPh	0.008	56
47	3-Pyr	A	NHPh	0.009	67
48	5-Pyrim	B	NHPh(4-Cl)	0.010	34
49	3-Pyr	C	O*t*Bu	0.017	56
50	3-Pyr	B	O*t*Bu	0.020	43
51	5-Pyrim	A	NHPh(4-Cl)	0.022	59
52	5-Pyrim	B	O*t*Bu	0.024	64
53	5-Pyrim	B	NH*t*Bu	0.054	>100
54	3-Pyr	A	NMe_2	0.120	>100
55	5-Pyrim	C	NHcPr	>1	>100
56	3-Pyr	E	NHcPr	>1	>100

[a] HET: 3-pyr (3-pyridine), 5-pyrim (5-pyrimidine).
[b] A (4-chlorophenyl), B (4-chloro-2-fluorophenyl), C (4-trifluoromethylphenyl), D (2-fluoro-4-trifluoromethylphenyl), E (4-benzonitrile), F (4-*i*propoxyphenyl).
[c] Tc = *T. cruzi*, values are the mean of at least two experiments.
[d] L6 cells (rat myoblasts from skeletal muscle) for assessment of cytotoxicity.

Table 4
R^1 = aryl (Ar)

Cmpd	HET[a]	R^{2b}	Ar	Tc IC_{50}[c] (μM)	L6 IC_{50}[d] (μM)
57	3-Pyr	D	Het[e]	0.017	51
58	3-Pyr	B	Ph	0.018	58
59	3-Pyr	A	Ph(2-OMe)	0.020	61
60	3-Pyr	B	2-pyrimidine	0.026	59
61	3-Pyr	F	Ph(2-OMe)	0.028	77
62	3-Pyr	A	Ph	0.034	67
63	5-Pyr	E	2-thiazole	0.050	>100
64	5-Pyrim	B	Ph(2-OMe)	0.065	60
65	5-Pyrim	B	Ph	0.078	63
66	2-Pyra	C	Ph(2-OMe)	0.240	62

[a] HET: 3-pyr (3-pyridine), 5-pyrim (5-pyrimidine), 2-pyra (2-pyrazine).
[b] A (4-chlorophenyl), B (4-chloro-2-fluorophenyl), C (4-trifluoromethylphenyl), D (2-fluoro-4-trifluoromethylphenyl), E (4-benzonitrile), F (4-*i*propoxyphenyl).
[c] Tc = *T. cruzi*, values are the mean of at least two experiments.
[d] L6 cells (rat myoblasts from skeletal muscle) for assessment of cytotoxicity.
[e] **57** Het = 5-(3-methyl-1,2,4-oxadiazole).

set, aromatic carbamates and carbonates (Table 3) were potent and more active than even bulky, lipophilic *t*-butyl analogues and pyridyl and pyrimidinyl analogues were equipotent. No activity advantage of carbamate-NH vs carbonate-O or for 2-F containing R^2 analogues was evident within the most potent aryl derivatives **43–48**.

The R^1 equal to aryl (Table 4) series shared an activity level similar to the amide series. The set was very limited in scope, but quite electronically diverse analogues such as **57**, **58** and **60** were essentially equiactive suggestive of a flat SAR and thus non-optimal binding interactions. This can be understood by considering that the most active sulphonamide/carbonate/carbamate series have an aromatic ring extended into chemical space whereas the directly linked *N*-aryl analogues are shorter and linear and probably do not reach into the same binding pocket.

3.2. Assessment of in vitro ADME and CYP3A4 inhibition profiles

Alongside the assessment of activity, compounds were screened in vitro for oxidative stability in human liver microsomes (to assess the likelihood of rapid hepatic clearance limiting systemic exposure after oral administration), solubility at pH 6.5 in phosphate buffer and selectivity for *T. cruzi* over CYP3A4 (a potentially limiting characteristic of the azole series and important for minimising potential drug-drug interactions for combination therapy).[28] Results for selected compounds are shown in Table 5.

Table 5
Representative in vitro metabolism, solubility and CYP selectivity data

Cmpd	E_H[a]	Sol.[b]	CYP[c]	Cmpd	E_H[a]	Sol.[b]	CYP[c]
24	<0.2	>100	7.4	**28**	0.71	<1.6	0.6
15	0.59	50–100	1.8	**35**	0.74	25–50	1
22	0.63	25–50	7	**36**	0.76	12.5–25	0.81
19	0.65	50–100	2.8	**29**	0.79	<1.6	1.9
14	0.66	12.5–25	3.9	**34**	0.84	25–50	5.6
17	0.68	12.5–25	2.3	**48**	0.56	3.1–6.3	0.3
13	0.73	12.5–25	1	**53**	0.69	50–100	6.9
16	0.89	6.3–12.5	3.9	**50**	0.75	3.1–6.3	1.9
39	0.53	12.5–25	3.6	**52**	0.76	12.5–25	2.9
37	0.65	12.5–25	1.3	**66**	0.9	3.1–6.3	25

[a] Microsome predicted hepatic extraction ratio (E_H) calculated from in vitro data in human liver microsomes.
[b] kinetic solubility at pH 6.5 in phosphate buffer (μg/mL) determined by nephelometry.
[c] IC_{50} (μM) for the inhibition of testosterone-β-hydroxylation by CYP3A4.

As is often the case, the most active compounds do not necessarily possess the best 'drug-like' properties. From the amide series, methyl analogue **24** (*T. cruzi* IC50 240 nM) was very stable to oxidation by microsomes, had excellent solubility and only moderate activity at CYP3A4. Higher alkyl and more active analogues **15**, **19**, **14** and **17** (*T. cruzi* $IC_{50} \leq 40$ nM) had acceptable profiles. The very active benzenesulfonyl analogues **28** and **29** (*T. cruzi* IC_{50}<10 nM) had disappointing profiles with Eh >0.7 suggesting they would have poor exposure profiles in vivo. Carbamates/carbonates **48, 53, 50** and **52** had mixed profiles with no clear standout compounds, whilst compounds in the aryl series were highly metabolised and poorly soluble (data not shown). Pyrazinyl analogue **66** had minimal cross-reactivity with CYP3A4, but was 10-fold less active than leading pyridyl compounds and thus of no real interest. Not enough comparative data was collected to determine the influence of R^2 on in vitro ADME and physicochemical properties, but previous studies with the triaryl series showed that the rate of oxidative metabolism could be reduced by the inclusion of 4-trifluoromethylphenyl.[25]

3.3. Evaluation of oral exposure

The systemic exposures of **24** and **37** (citrate salt) were determined in non-infected male Swiss outbred mice after single oral doses of 20, 50 and 100 mg/kg administered by gavage. Both compounds exhibited rapid absorption after oral administration, with maximum concentrations attained approximately 15 min post-dose. No adverse reactions or compound-related side effects were observed following oral administration of either compound at the dose levels examined. The apparent half-lives of **37** ($T_{1/2}$ = 2.1–2.9 h) and **24** ($T_{1/2}$ = 1.7–2.7 h) were similar, however the AUC for **37** over the 7.5 h post-dose sampling period was higher than that for **24** at each comparable dose (**37**: $AUC_{0-7.5\ h}$ (μM h) 7.2 at 20 mg/kg, 60.2 at 50 mg/kg and 43.7 at 100 mg/kg. **24**: $AUC_{0-7.5\ h}$ (μM h) 2.3 at 20 mg/kg, 6.2 at 50 mg/kg and 9.4 at 100 mg/kg) (see Supplementary data for oral exposure profiles). Full-scan LC-MS data were collected for selected plasma samples to identify potential metabolites. Putative products of oxygenation and amide hydrolysis were detected for **24**, and products of oxygenation and N-dealkylation were observed for **37**. Potential metabolites having molecular weights consistent with the products of glucuronidation, sulphation or oxygenation followed by conjugation or ring opening were not detected.

3.4. Evaluation of in vivo efficacy

Compounds **24** and **37** were evaluated for in vivo efficacy in a mouse model of acute *T. cruzi* infection following doses of 20, 50 and 100 mg/kg. Female Swiss mice (n = 5 per group) were infected with 25,000 blood form trypomastigotes of *T. cruzi* (Tulahuen strain/Tc VI). Compound dosing commenced on day 8 post infection (pi) and each mouse received the indicated dosage of compound in a single, once daily administration by oral gavage for 5 consecutive days. Blood parasitemia was evaluated on days 8, 9, 12 and 14 pi and expressed as 'number of trypomastigotes/mL of blood'. Compound efficacy was indicated by a decrease in parasitemia levels in comparison to vehicle-treated mice on day 14 pi.

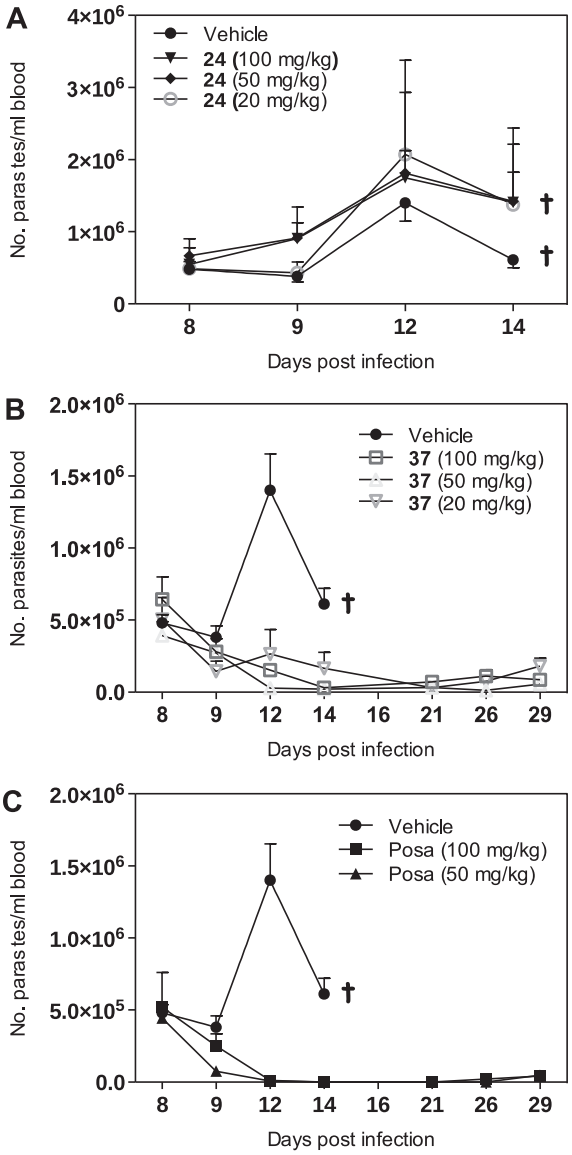

Figure 3. Efficacy of compounds on blood parasitemia in vivo. Animals were administered (A) **24**, (B) **37** or (C) posaconazole once daily for 5 days at different concentrations. Parasitemia per ml blood was evaluated relative to vehicle-treated animals. † indicates animal death due to parasite burden/morbidity. Error bars represent SEM.

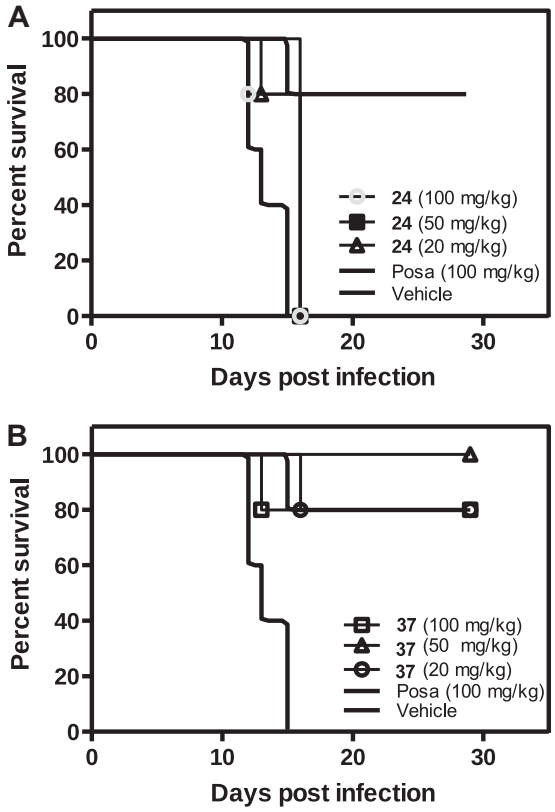

Fig. 4. Survival following compound treatment. Animals were administered (A) **24** or (B) **37** once daily for 5 days at different concentrations. Percent survival relative to treatment with posaconazole (100 mg/kg) or vehicle only is shown.

Posaconazole (Noxafil®) treated mice (50 and 100 mg/kg) were used as a positive control alongside the vehicle only treated group.

Compared to vehicle-treated mice, **24** was unable to significantly reduce blood parasitemia at all doses tested (Fig. 3A) but was able to improve survival. All **24**-treated mice survived to the end of the treatment period (day 14) whereas 60% of vehicle-treated mice did not survive past day 12 (Fig. 4A). In contrast, **37**-treated mice had significantly improved reduction in parasitemia when dosed at 100, 50 and 20 mg/kg (96%, 95% and 73%) compared to vehicle-treated on day 14, respectively) (Fig. 3B). All **37**-treated mice had improved survival outcomes relative to vehicle (4:5 mice at 20 mg/kg; 5:5 at 50 mg/kg and 4:5 at 100 mg/kg survived to the end of the experiment) (Fig. 4B). This was comparable to the positive control, posaconazole, which reduced blood parasitemia to below detectable limits by day 14 pi in both 50 mg/kg and 100 mg/kg treated groups (Fig. 3C), with 3:5 mice (50 mg/kg) and 4:5 mice (100 mg/kg) surviving to the end of the experiment (Fig. 4).

4. Conclusions

Simple 1-[phenyl(pyridin-3-yl)methyl]piperazinyl analogues of fenarimol were investigated for their ability to inhibit *T. cruzi* in vitro in a whole parasite assay and further studied for in vivo efficacy in a mouse model of acute *T. cruzi* infection. A range of analogues bearing amide, sulfonamide, carbamate/carbonate and aryl substituents appended to [phenyl(pyridin-3-yl)methyl]piperazine scaffolds **3** exhibited low nM activities in vitro. Two compounds, **24** and **37**, gave good plasma exposures in mice following oral admin-

istration and were tested for efficacy in vivo. Compound **37** was able to significantly reduce parasitemia in a mouse model of acute *T. cruzi* infection after once daily oral dosing at 20, 50 and 100 mg/kg for 5 days, consistent with a higher potency and overall superior plasma concentration profile compared to **24** which was not efficacious in vivo. The tractable synthesis of the target compounds, oral exposure profiles and demonstrated in vivo efficacy of **37** makes the 1-[phenyl(pyridin-3-yl)methyl]piperazinyl series an attractive target for further optimisation.

5. Experimental

5.1. General

Reagents were purchased from commercial suppliers and used without further purification. Commercially available anhydrous solvents were used and stored under nitrogen, unless indicated otherwise. Reactions involving moisture sensitive reagents were conducted under an atmosphere of dry nitrogen in glassware dried with a heat-gun. Thin layer chromatography (TLC) using silica gel Merck 60 F254 plates and detection with UV light was used to monitor reactions. ^{1}H NMR spectra were recorded in $CDCl_3$, CD_3OD or DMSO-*d6* solutions on a Varian 200, Brucker 300 or Varian 400 MHz machine. Chemical shifts are reported in parts per million (δ) downfield of tetramethylsilane (TMS). GC–MS were acquired on an Agilent 5973 network machine. LC-MS were acquired on an Applied Biosystems/MDS Sciex API-2000 system. Flash chromatography was carried out with silica gel (0.04–0.06 μm, 230–400 mesh), reverse phase silica gel (C18 35-70 μm) or on a Flashmaster II system using cartridges prepared in-house. Microwave irradiations were conducted using a Biotage initiator. All compounds tested in the in vitro and in vivo biological screens were purified to ≥95% purity as determined by analysis of HPLC on an Agilent 1100 series machine, fitted with a C8 reverse phase Agilent zorbax eclipse DB-LB 4.6 x 150 mm 5 μm column (flow rate 1.2 mL/min; method 1: 20% acetonitrile in water, increasing to 60% acetonitrile over 10 min; method 2: 50% acetonitrile in water increasing to 90% acetonitrile over 10 min; method 3: 70% acetonitrile in water increasing to 95% acetonitrile over 10 min); ^{1}H NMR spectra (accounting for non-compound peaks and residual solvent) and in some cases LC-MS or GC–MS. Fenarimol [60168-88-9] (**1**) was purchased from commercial sources and posaconazole was a gift from the CDCO.

5.2. Synthesis of compounds

The preparation of [4-chlorophenyl(pyridin-3-yl)methyl]piperazine analogues **24**, **29**, **46**, **47** and **62** is provided as a representative example of the synthetic methodology. The synthesis of compound **37** is also described. Methods and data for other reported compounds is available in the Supplementary data.

5.2.1. Preparation of diarylmethanol intermediates (6) from benzophenones[25]

5.2.1.1. (4-Chlorophenyl)(pyridin-3-yl)methanol (9). To a solution of 3-(4-chlorobenzoyl)pyridine (3 g, 14 mmol) in methanol (20 mL) was slowly added sodium borohydride (0.72 g, 20 mmol). The mixture was stirred at room temperature under nitrogen for 48 h, then concentrated, diluted with water (40 mL) and extracted with chloroform (40 mL). The organic layer was dried, filtered and the filtrate concentrated to afford **9** as a white solid (3 g, 97%). ^{1}H NMR (300 MHz, CHLOROFORM-*d*) δ 8.54 (d, J = 2.0 Hz, 1H), 8.46 (dd, J = 4.8, 1.4 Hz, 1H), 7.60–7.76 (m, 1H), 7.21–7.36 (m, 5H), 5.85 (d, J = 2.3 Hz, 1H), 3.27 (br s, 1H).

5.2.2. Preparation of chloro diarylmethyl intermediates (7) from diarylmethanol intermediates (6)

5.2.2.1. 3-[Chloro(4-chlorophenyl)methyl]pyridine (10). A mixture of **9** (2.5 g, 11 mmol), thionyl chloride (5.2 g, 44 mmol) and toluene or dichloromethane (10 mL) was stirred at room temperature for 2 h with a drying tube or heated under reflux overnight. On cooling, the mixture was concentrated and azeotroped with toluene (2 × 10 mL) to afford **10** as a white solid (2.5 g, 94%). ^{1}H NMR (300 MHz, CHLOROFORM-*d*) δ 8.63 (d, J = 2.0 Hz, 1H), 8.57 (dd, J = 4.7, 1.3 Hz, 1H), 7.69–7.76 (m, 1H), 7.24–7.39 (m, 5H), 6.11 (s, 1H).

5.2.3. Preparation of diarylmethylpiperazine intermediates (4 and 5) from chloro diarylmethyl intermediates (7)

5.2.3.1. 1-[(4-Chlorophenyl)(pyridin-3-yl)methyl]piperazine (12). To a dry 100 mL round bottomed flask fitted with a condenser and a stirrer bar was added **10** (5 g, 21 mmol). This was dissolved in anhydrous acetonitrile (40 mL) and *t*-butyl piperazine-1-carboxylate (5.9 g, 31.5 mmol) was added followed by triethylamine (anhydrous, 5.9 mL, 42 mmol) and a catalytic amount of potassium iodide (dried by heat-gun under vacuum). The reaction was heated at 80 °C for 48 h. The reaction mixture was cooled, concentrated and the residue partitioned between dichloromethane (100 mL) and a saturated aqueous sodium carbonate solution (100 mL). The aqueous phase was re-extracted with dichloromethane (2 × 50 mL), the organic phases combined, dried (sodium sulfate), filtered and concentrated to give a crude orange oil. Purification by Flashmaster II chromatography (eluent ethylacetate in dichloromethane 0–30%) gave BOC-intermediate **11** as a semi-pure solid (16.1 g, 80%). ^{1}H NMR (400 MHz, CHLOROFORM-*d*) δ 8.62 (br s, 1H), 8.47 (d, J = 3.9 Hz, 1H), 7.68 (d, J = 7.8 Hz, 1H), 7.17–7.38 (m, 5H), 4.28 (s, 1H), 3.36–3.48 (m, 4H), 2.25–2.39 (m, 4H), 1.43 (s, 9H). **11** (3.4 g, 8.8 mmol) was dissolved in dichloromethane (40 mL) and methanol (10 drops) was added. The mixture was cooled to 0 °C and trifluoroacetic acid (6.5 mL, 87.7 mmol) was added drop wise. The mixture was stirred for 1 h at 0 °C, allowed to come to room temperature overnight, concentrated and azeotroped with dichloromethane to give **12** (3.7 g) as the crude trifluoroacetic acid salt which was used without further purification. ^{1}H NMR (400 MHz, DMSO-d_6) δ 8.87 (br s, 1H), 8.64–8.77 (m, 2H), 8.32 (d, J = 7.8 Hz, 1H), 7.81 (dd, J = 7.6, 5.7 Hz, 1H), 7.39–7.48 (m, 4H), 4.86 (s, 1H), 3.13 (br. s., 4H), 4 protons obscured by DMSO peak.

5.2.4. Preparation of diarylmethylpiperazine analogue libraries (3) from diarylmethylpiperazine intermediates (5) method A

5.2.4.1. Amides from acid chlorides. 1-{4-[(4-Chlorophenyl)(pyridin-3-yl)methyl]piperazin-1-yl}ethan-1-one (24). Compound **12** (3.7 g) was dissolved in anhydrous dichloromethane (30 mL) and the solution cooled to 0 °C. Triethylamine (5 mL, 36 mmol) was added drop wise with stirring. A further 5 mL of triethylamine was added, followed by drop wise addition of acetyl chloride (1.0 mL, 14.4 mmol) and the mixture allowed to stir for 45 min, poured onto aqueous sodium carbonate solution (20 mL) and extracted with chloroform (3 × 40 mL). The organic phases were combined, dried (sodium sulfate), filtered and concentrated to give a dark orange oil which was purified by Flashmaster II chromatography (eluent chloroform in methanol) to give **24** (485 mg, 17%) as a hygroscopic colourless solid. ^{1}H NMR (300 MHz, CHLOROFORM-*d*) δ 8.64 (br s, 1H), 8.49 (d, J = 2.4 Hz, 1H), 7.71 (d, J = 7.9 Hz, 1H), 7.19–7.40 (m, 5H), 4.30 (s,

1H), 3.62 (apparent triplet, J = 4.9 Hz, 2H), 3.47 (apparent triplet, J = 4.9 Hz, 2H), 2.28–2.48 (m, 4H), 2.06 (s, 3H); HPLC 96.1% at 230 nm; GCMS m/z = 329.

5.2.4.2. Sulfonamides from sulfonyl chlorides. 1-(Benzenesulfonyl)-4-[(4-chlorophenyl)(pyridin-3-yl)methyl]piperazine (29). Compound **12** (250 mg, 0.24 mmol) was dissolved in dichloromethane (2.5 mL) under an atmosphere of nitrogen and benzenesulfonyl chloride (0.46 mL, 2 equiv) was added and the mixture cooled to 0 °C. Triethylamine (0.6 mL) was added and the mixture stirred for 2 h then allowed to warm to room temperature, poured onto a saturated aqueous sodium carbonate solution (20 mL) and extracted with dichloromethane (3 × 15 mL). The organic phases were combined, dried (magnesium sulfate), filtered, concentrated and purified by Flashmaster II chromatography (eluent ethylacetate in dichloromethane) to give **29** as an off-white powder (86 mg, 83%). ^{1}H NMR (300 MHz, CHLOROFORM-*d*) δ 8.57 (br s, 1H), 8.45 (br s, 1H), 7.74–7.78 (m, 2H), 7.54–7.68 (m, 4H), 7.24–7.26 (m, 4H) 7.16–7.22 (m, 1H), 4.28 (s, 1H) 3.02–3.05 (m, 4H), 2.44–2.48 (m, 4H); HPLC >99% at 230 nm; LCMS $[M+H]^+$ = 428.2.

5.2.4.3. Carbonates from chloroformates. Phenyl 4-[(4-chlorophenyl)(pyridin-3-yl)methyl]piperazine-1-carboxylate (46). A solution of **12** (0.3 g) in dichloromethane (3 mL) was cooled to 0 °C and triethylamine (1.5 mL) was added, followed by phenyl chloroformate (0.07 mL, 0.58 mmol). The mixture was allowed to warm to room temperature overnight, then 10 mL of a saturated solution of ammonium chloride and 10 mL of dichloromethane were added. The organic phase was separated and the aqueous phase re-extracted with dichloromethane (2 × 10 mL). The organic phases were combined, dried (magnesium sulfate) filtered and concentrated. The crude material was purified by Flashmaster II chromatography (eluent ethyl acetate in hexanes) to give **46** (66 mg, 56%) as an off-white solid. ^{1}H NMR (400 MHz, CHLOROFORM-*d*) δ 8.66 (br s., 1H), 8.50 (br s., 1H), 7.71 (d, J = 7.8 Hz, 1H), 7.23–7.40 (m, 7H), 7.20 (d, J = 7.0 Hz, 1H), 7.09 (d, J = 8.2 Hz, 2H), 4.34 (s, 1H), 3.50–3.79 (m, 4H), 2.34–2.55 (m, 4H); HPLC 96.9% at 230 nm; LCMS $[M+H]^+$ = 408.1.

5.2.4.4. Carbamates from isocyanates. 4-[(4-Chlorophenyl)(pyridin-3-yl)methyl]-N-phenylpiperazine-1-carboxamide (47). Compound **12** (0.3 g, 0.29 mmol) was dissolved in dichloromethane (3.0 mL) and the solution was cooled to 0 °C. Triethylamine (2.0 mL) was added, followed by phenyl isocyanate (52 mg, 0.44 mmol) and the mixture stirred for 30 min, poured into a saturated solution of sodium chloride (20 mL) and extracted with dichloromethane (2 × 10 mL). The organic phases were combined, dried (magnesium sulfate) filtered and concentrated. The crude material was purified by Flashmaster II chromatography (eluent ethyl acetate in hexanes) to give **47** (83 mg, 70%) as a white solid. ^{1}H NMR (400 MHz, DMSO-d_6) δ 8.63 (s, 1H), 8.40–8.52 (m, 2H), 7.81 (d, J = 7.8 Hz, 1H), 7.48 (d, J = 8.6 Hz, 2H), 7.39–7.44 (m, 3H), 7.36 (dd, J = 7.6, 4.9 Hz, 1H), 7.21 (t, J = 7.8 Hz, 2H), 6.92 (t, J = 7.2 Hz, 1H), 4.54 (s, 1H), 3.42–3.52 (m, 4H), 2.23–2.38 (m, 4H); HPLC >99% at 230 nm; LCMS $[M+H]^+$ = 407.3.

5.2.4.5. Aryl derivatives. 1-[(4-Chlorophenyl)(pyridin-3-yl)methyl]-4-phenylpiperazine (62). A mixture of **10** (0.20 g, 0.7 mmol), *N*,*N*-dimethylformamide (2 mL), potassium carbonate (0.5 g, 2.1 mmol) and 1-phenylpiperazine (0.57 g, 3.5 mmol) was heated at 150 °C for 30 min in a microwave. The mixture was diluted with water (40 mL) and extracted into ethyl acetate (40 mL). The organic layer was separated, washed with water (40 mL), dried, and concentrated. The crude residue was purified by Flashmaster II chromatography to give **62** (60 mg, 24%) as a clear oil. ^{1}H NMR (300 MHz, CHLOROFORM-*d*) δ 8.61–8.75 (m, 1H), 8.42–8.56 (m, 1H), 7.68–7.85 (m, 1H), 7.20–7.42 (m, 7H), 6.76–7.00 (m, 3H), 4.34 (s, 1H), 3.17–3.28 (m, 4H), 2.47–2.67 (m, 4H); HPLC >99% at 230 nm; GCMS m/z = 363.

5.2.5. Preparation of 1-[(4-chloro-2-fluorophenyl)(pyridin-3-yl)methyl]-4-methanesulfonylpiperazine (37). (4-Chloro-2-fluorophenyl)(pyridin-3-yl)methanol (67)

To a solution of (4-chloro-2-fluorochlorophenyl)(pyridin-3-yl)-methanone (15.6 g, 66.2 mmol) in methanol (400 mL) cooled to 0 °C was slowly added sodium borohydride (4.5 g, 119 mmol) portion wise. The mixture was stirred at room temperature under nitrogen for 24 h, then diluted with water (400 mL) and extracted into dichloromethane (4 × 300 mL). The organic layer was dried, filtered and concentrated. Purification by silica plug (eluent dichloromethane then ethyl acetate) gave **67** as a white powder (11.3 g, 72%). ^{1}H NMR (300 MHz, CHLOROFORM-*d*) d 8.60 (d, J = 2.1 Hz, 1H), 8.48 (dd, J = 4.8, 1.8 Hz, 1H), 7.71–7.67 (m, 1H), 7.50 (t, J = 8.1 Hz, 1H), 7.29–7.25 (m, 1H), 7.20–7.17 (m, 1H), 7.07 (dd, J = 9.9, 1.8 Hz, 1H), 6.13 (d, J = 3.4 Hz, 1H), 3.05 (d, J = 3.4 Hz, 1H); HPLC >99% @230 nm.

5.2.5.1. 3-[Chloro(4-chloro-2-fluorophenyl)methyl]pyridine (68). A solution of **67** (11.3 g, 47.5 mmol) in dichloromethane (140 mL) was cooled to 0 °C and thionyl chloride (5.86 mL, 80.8 mmol) added. The reaction mixture was allowed to warm to room temperature over 2 h. The mixture was concentrated, re-extracted into dichloromethane and washed with an aqueous solution of sodium carbonate. The aqueous layer was treated with salt and re-extracted with dichloromethane (3 × 100 mL). The organic layers were combined, dried (magnesium sulfate), filtered and concentrated to give **68** as a crude light brown oil (11.2 g, 93%). ^{1}H NMR (300 MHz, CHLOROFORM-*d*) d 8.65 (s, 1H), 8.56 (d, J = 3.6, 1H), 7.78–7.74 (m, 1H), 7.49 (t, J = 8.4 Hz, 1H), 7.32 (dd, J = 8.1, 4.8 Hz, 1H), 7.22–7.18 (m, 1H), 7.12 (dd, J = 8.1, 1.8 Hz, 1H), 6.37 (s, 1H).

5.2.5.2. 1-[(4-Chloro-2-fluorophenyl)(pyridin-3-yl)methyl]piperazine (69). Compound **68** (11.2 g, 43.7 mmol) was dissolved in anhydrous acetonitrile (100 mL) and *t*-butyl piperazine-1-carboxylate (24.4 g, 0.13 mmol) was added followed by triethylamine (anhydrous, 12.2 mL, 87.4 mmol) and a catalytic amount of potassium iodide (dried by heat gun under vacuum). The reaction was heated at 80 °C for 48 h (an additional 12 mL triethylamine and 5 g of *t*-butyl piperazine-1-carboxylate were added after 24 h). The reaction mixture was cooled, concentrated and the residue partitioned between dichloromethane (100 mL) and a saturated solution of sodium carbonate (100 mL). The aqueous phase was re-extracted with dichloromethane (3x100 mL), the organic phases combined, dried (sodium sulfate), filtered and concentrated to give a crude off-white solid (16.3 g, 92%). The crude material (4 g, 9.85 mmol) was dissolved in dichloromethane (40 mL) and methanol (1 mL) was added. The mixture was cooled to 0 °C and trifluoroacetic acid (10 mL, 135 mmol) was added drop wise. The mixture was stirred for 4 days, concentrated and azeotroped with dichloromethane to give **69** (8.5 g) as the crude trifluoroacetic acid salt as an orange oil which was used without further purification. ^{1}H NMR (200 MHz, CHLOROFORM-*d*) (Free base) δ 8.64 (s, 1H), 8.42–8.51 (m, 1H), 7.69 (br d, J = 7.7 Hz, 1H), 7.52 (t, J = 8.1 Hz, 1H), 7.17–7.29 (m, 1H), 7.09–7.17 (m, 1H), 7.03 (dd, J = 1.8, 9.9 Hz, 1H), 4.68 (s, 1H), 2.84–3.03 (m, 4H), 2.32–2.52 (m, 4H).

5.2.5.3. 1-[(4-Chloro-2-fluorophenyl)(pyridin-3-yl)methyl]-4-methanesulfonylpiperazine (37). Compound **69** (5 g, 5.8 mmol) was dissolved in a solution of dichloromethane (40 mL)

containing triethylamine (5 mL) at 0 °C. Methanesulfonyl chloride (0.9 mL, 11.6 mmol) was added drop wise and the mixture stirred for 2 h then allowed to warm to room temperature, poured onto a saturated solution of ammonium chloride (20 mL) and extracted with dichloromethane (3 × 30 mL). The organic phases were combined, dried (magnesium sulfate), filtered, concentrated and purified by preparative HPLC (eluent 30% acetonitile in water) to give **37** as an off-white solid (690 mg, 31%). ^{1}H NMR (300 MHz, CHLOROFORM-*d*) δ 8.64–8.68 (m, 1H), 8.48–8.54 (m, 1H), 7.63–7.72 (m, 1H), 7.47 (t, J = 8.0 Hz, 1H),7.21–7.25 (m, 1H), 7.11–7.18 (m, 1H), 7.02–7.10 (m, 1H), 4.76 (s, 1H), 3.27 (apparent triplet, J = 4.8 Hz, 4H), 2.81 (s, 3H), 2.44–2.62 (m, 4H); HPLC 97.4% at 230 nm; LCMS $[M+H]^+$ = 384.1.

5.3. Biological assays

General methods for the in vitro *T. cruzi* assay for determination of IC_{50}, in vitro assay for determination of cytotoxicity, solubility, microsomal stability, cytochrome P450 3A4/5 and in vivo efficacy model of acute *T. cruzi* infection in mice as previously described.[25]

Acknowledgments

DND*i* is grateful to its donors, public and private, who have provided funding to DND*i* since its inception in 2003. With the support of these donors, DND*i* is well on its way to achieving the objectives of building a robust pipeline and delivering 6–8 new treatments by 2014. A full list of DND*i*'s donors can be found at http://www.dndi.org/index.php/donors.htmL?ids=8. For the work described in this paper, DND*i* received financial support from the following donors: Department for International Development (DFID)/UNITED KINGDOM, GiZ on behalf of the Government of the Federal Republic of Germany/GERMANY, Ministry of Foreign and European Affairs (MAEE)/FRANCE, Spanish Agency for International Development Cooperation (AECID)/SPAIN, Swiss Agency for Development and Cooperation (SDC)/SWITZERLAND, Medecins Sans Frontieres (Doctors without Borders)/INTERNATIONAL and a Swiss foundation. The donors had no role in study design, data collection and analysis, decision to publish, or preparation of the manuscript.

The authors thank Harriet Newson and Sarah Keatley for help in preparing the manuscript and Jason Chaplin and Michael Abbott for additional chemistry support.

Supplementary data

Supplementary data (additional synthetic methods for the preparation of intermediates to final compounds, spectroscopic/analytical data and oral exposure profiles for **24** and **37** is available) associated with this article can be found, in the online version, at http://dx.doi.org/10.1016/j.bmc.2013.01.050.

References and notes

1. *Nature Outlook* 2010, 24th June.
2. Hotez, P. J.; Dumonteil, E.; Woc-Colburn, L.; Serpa, J. A.; Bezek, S.; Edwards, M. S.; Hallmark, C. J.; Musselwhite, L. W.; Flink, B. J.; Bottazzi, M. E. *PLoS Negl. Trop. Dis.* **2012**, *6*, e1498.
3. Andrade, L. O.; Andrews, N. W. *Nat. Rev. Microbiol.* **2005**, *3*, 819.
4. Cencig, S.; Coltel, N.; Truyens, C.; Carlier, Y. *PLoS Negl. Trop. Dis.* **2011**, *5*, e1216.
5. Bern, C. *N. Eng. J. Med.* **2011**, *364*, 2527.
6. Martins-Melo, F.; Alencar, C. H.; Ramos, A. N., Jr.; Heukelbach, J. *PLoS Negl. Trop. Dis.* **2012**, *6*, e1508.
7. Moolani, Y.; Bukhman, G.; Hotez, P. J. *PLoS Negl. Trop. Dis.* **2012**, *6*, e1499.
8. Zingales, B.; Miles, M. A.; Campbell, D. A.; Tibayrenc, M.; Macedo, A. M.; Teixeira, M. M. G.; Schijman, A. G.; Llewellyn, M. S.; Lages-Silva, E.; Machado, C. R.; Andrade, S. G.; Sturm, N. R. *Infect. Genet. Evol.* **2012**, *12*, 240.
9. Lepesheva, G. I.; Hargrove, T. Y.; Kleshchenko, Y.; Nes, D. W.; Villalta, F.; Waterman, M. R. *Lipids* **2008**, *43*, 1117.
10. Lepesheva, G. I.; Waterman, M. R. *Biochim. Biophys Acta* **2007**, *1770*, 467.
11. Urbina, J. A. *Curr. Pharm. Des.* **2002**, *8*, 287.
12. Urbina, J. A.; Docampo, R. *Trends Parasitol.* **2003**, *19*, 495.
13. Urbina, J. A.; Payares, G.; Sanoja, C.; Lira, R.; Romanha, A. J. *Int. J. Antimicrob. Agents* **2003**, *21*, 27.
14. Diniz, L.; Caldas, I. S.; Guedes, P. M. D. M.; Crepalde, G.; de Lana, M.; Carneiro, C. M.; Talvani, A.; Urbina, J. A.; Bahia, M. T. *Antimicrob. Agents Chemother.* **2010**, *54*, 2979.
15. Buckner, F. S.; Bahia, M. T.; Suryadevara, P. K.; White, K. L.; Shackleford, D. M.; Chennamaneni, N. K.; Hulverson, M. A.; Laydbak, J. U.; Chatelain, E.; Scandale, I.; Verlinde, C. L. M. J.; Charman, S. A.; Lepesheva, G. I.; Gelb, M. H. *Antimicrob. Agents Chemother.* **2012**, *56*, 4914.
16. Kraus, J. M.; Tatipaka, H. B.; McGuffin, S. A.; Chennamaneni, N. K.; Karimi, M.; Arif, J.; Verlinde, C. L. M. J.; Buckner, F. S.; Gelb, M. H. *J. Med. Chem.* **2010**, *53*, 3887.
17. Kraus, J. M.; Verlinde, C. L. M. J.; Karimi, M.; Lepesheva, G. I.; Gelb, M. H.; Buckner, F. S. *J. Med. Chem.* **2009**, *52*, 1639.
18. Hucke, O.; Gelb, M. H.; Verlinde, C. L. M. J.; Buckner, F. S. *J. Med. Chem.* **2005**, *48*, 5415.
19. Suryadevara, P. K.; Olepu, S.; Lockman, J. W.; Ohkanda, J.; Karimi, M.; Verlinde, C. L. M. J.; Kraus, J. M.; Schoepe, J.; Van Voorhis, W. C.; Hamilton, A. D.; Buckner, F. S.; Gelb, M. H. *J. Med. Chem.* **2009**, *52*, 3703.
20. Doyle, P. S.; Chen, C.; Johnston, J. B.; Hopkins, S. D.; Leung, S. S. F.; Jacobson, M. P.; Engel, J. C.; McKerrow, J. H.; Podust, L. M. *Antimicrob. Agents Chemother.* **2010**, *54*, 2480.
21. Konkle, M. E.; Hargrove, T. Y.; Kleshchenko, Y. Y.; von Kries, J. P.; Ridenour, W.; Uddin, J. M.; Caprioli, R. M.; Marnett, L. J.; Nes, W. D.; Villalta, F.; Waterman, M. R.; Lepesheva, G. I. *J. Med. Chem.* **2009**, *52*, 2846.
22. Gunatilleke, S. S.; Calvet, C. M.; Johnston, J. B.; Chen, C.; Erenburg, G.; Gut, J.; Engel, J. C.; Ang, K. K. H.; Mulvaney, J.; Chen, S.; Arkin, M. R.; McKerrow, J. H.; Podust, L. M. *PLoS Negl. Trop. Dis.* **2012**, *6*, e1736.
23. Lepesheva, G. I.; Hargrove, T. Y.; Anderson, S.; Kleshchenko, Y.; Furtak, V.; Wawrzak, Z.; Villalta, F.; Waterman, M. R. *J. Biol. Chem.* **2010**, *33*, 25582.
24. Chen, C.; Leung, S. S. F.; Guilbert, C.; Jacobson, M. P.; McKerrow, J. H.; Podust, L. M. *PLoS Negl. Trop. Dis.* **2010**, *4*, e651.
25. Keenan, M.; Abbott, M. J.; Alexander, P. W.; Armstrong, T.; Best, W. M.; Berven, B.; Botero, A.; Chaplin, J. H.; Charman, S. A.; Chatelain, E.; von Geldern, T. W.; Kerfoot, M.; Khong, A.; Nguyen, T.; McManus, J. D.; Morizzi, J.; Ryan, E.; Scandale, I.; Thompson, R. A.; Wang, S. Z.; White, K. L. *J. Med. Chem.* **2012**, *55*, 4189.
26. Buckner, F. S.; Verlinde, C. L.; La Flamme, A. C.; Van Voorhis, W. C. *Antimicrob. Agents Chemother.* **1996**, *40*, 2592.
27. http://www.FRAC.Info.
28. Cronin, S.; Chandrasekar, P. H. *J. Antimicrob. Chemother.* **2010**, *65*, 410–416.